Crystal-structure stabilities and electronic structure for the light actinides Th, Pa, and U

J. M. Wills and Olle Eriksson

Center for Materials Science and Theoretical Division, Los Alamos National Laboratory, Los Alamos, New Mexico 87545

(Received 9 September 1991)

The crystal-structure stabilities, equilibrium volumes, and bulk moduli (at $T=0$) of the light actinides Th, Pa, and U, have been calculated by means of full-potential, total-energy band-structure calculations. The total energies of the three elements were calculated as a function of volume in the three experimentally observed crystal structures: fcc, bct, and orthorhombic (α-U). Our calculations reproduce the experimentally observed crystal structures, as well as the equilibrium volumes and bulk moduli (the bulk modulus of Pa being an exception). Other calculated ground-state properties are also in good agreement with experiment, e.g., crystal-structure parameters (c/a ratio and positional parameters). On the basis of our results, we argue that the $5f$ electrons are participating in the chemical bonds, and that they have a large influence on the crystal structure. The equilibrium volumes of hypothetical fcc structures are found to show increasing deviations from the volumes obtained in the true crystal structures, as the $5f$ band becomes filled. Also, these fully relativistic calculations (assuming a fcc structure) show a smaller volume for Pu than for Np, in contrast to the experimental finding. We therefore propose that the anomalous volume of α-Pu is associated with its very unusual crystal structure, rather than with relativistic effects. Detailed information from the calculations is presented, such as the density of states, charge-density contour plots, and orbital occupation numbers.

I. INTRODUCTION

It was realized in the 1940s that the elements with a nuclear charge larger than in actinium ($Z=89$) form a series of their own, which was named the actinide series.[1] Due to the similarity of the volumes between the early actinides and the transition metals (Fig. 1) it was suggested that the light actinides were part of a $6d$ series.[2] Since the volume of americium (Am) is much larger than the element preceding it, plutonium (Pu), and is comparable to the volumes of the rare-earth elements (Fig. 1), it was further suggested that the $5f$ shell was chemically inert, and was starting to get filled in Am.[2] However, there are pronounced differences between the actinides and the transition metals. The latter have fcc, hcp, or bcc crystal structures, whereas the light actinides show much more complicated structures at low temperatures; Th (fcc), Pa (bct), U (orthorhombic, 2 atoms/unit cell), Np (orthorhombic, 8 atoms/unit cell), and Pu (monoclinic, 16 atoms/unit cell). Also, the melting temperatures are anomalous,[3] as are the thermal-expansion coefficients.[4] The trend of the bulk modulus, as well as the trend of the cohesive energy, for the light actinides is also quite different from the trend exhibited by the transition metals.[3]

A pioneering atomic calculation showed that the $5f$ wave function drops to low energies for uranium.[5] Similarly early energy-band calculations of light actinide elements showed that the $5f$ band was fairly broad, and pinned to the Fermi level (E_F).[6] Therefore, it was evi-
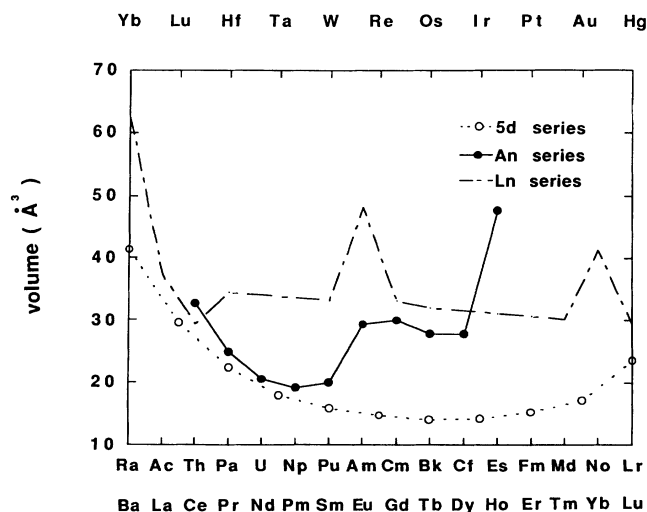

FIG. 1. Experimental data of the equilibrium volumes of the $5d$ series, the rare-earth series, and the actinide series (a similar figure was published in Ref. 12).

dent that the $5f$ electrons have to participate in the chemical bonding (explaining the parabolic trend of the volumes exhibited by the light actinides), and that the actinide series is a $5f$ series. Contrary to the rare-earth series, the $5f$ electrons of the light actinides are delocalized. This also explains why the light actinides show a lack of magnetic ordering, since the relatively broad $5f$ band prevents $5f$ localization or even band magnetism. The jump in volume between Pu and Am was suggested to be a Mott transition with the $5f$ electrons being nonbonding and localized in Am.[7] Americium was suggested to be trivalent, with an f^6 configuration, having a $J=0$ ground state.[7] Therefore, in agreement with experiments, Am is expected to be nonmagnetic and was even predicted to be superconducting,[8] which was later verified.[9]

The picture that has evolved[3] is that the light actinides (Th–Pu) have delocalized $5f$ electrons which participate in the chemical bonding, and that from Am on the $5f$ electrons are localized,[2,7,10] making the latter part of the actinide series similar to the rare-earth elements. The crystal structures of Am and the proceeding elements are also the same or very similar to the structures of the rare-earth elements. The hypothesis that the early actinides have delocalized $5f$ electrons was supported by self-consistent energy-band calculations (assuming a hypothetical fcc structure), which reproduced the experimental volumes,[10] as well as the cohesive energies.[11,12] It was also shown how relativistic effects quite dramatically influence the equilibrium volume,[11,12] as well as the electron-phonon coupling constant,[13] of Pu. Among many other peculiar properties (which we do not mention here), this makes Pu quite unique among the metallic elements of the Periodic Table.

If the $5f$ electrons are itinerant and pinned to E_F in the light actinides, one would expect to see a strong x-ray photoelectron (XPS) signal at E_F. This has also been observed and theoretical calculations of XPS intensities, assuming delocalized $5f$ electrons, reproduce these experiments.[14] Furthermore, non-self-consistent calculations[15] (again assuming delocalized $5f$'s) of Fermi surface topologies reproduce experimental data fairly well for uranium.[16]

Hence, it seems that there are, indeed, similarities of the microscopic properties between the early actinides and the transition metals, explaining some of the similarities of the macroscopic properties. For instance, the trend in the volumes can easily be explained with a simple Friedel model, where the transition metals have a a d band pinned at E_F and the actinides have an f band.[6,10–15] Since there are similarities in the electronic structure between the transition metals and the actinides, it is of interest to study why they have such different crystal structures, and especially to investigate whether the observed crystal structures are compatible with the general picture of the light actinides (itinerant $5f$ electrons). In this context it is interesting to note that the crystal structures of the transition metals[17] and rare-earth elements[18] (excluding Ce) have been determined with great accuracy, and were shown to be governed by the d electrons. Subsequent full-potential calculations showed essentially the same results.[19] It should also be men-

tioned here that Skriver[17] calculated the energy difference between the bcc and fcc structures for all the light actinides and found that, at zero temperature, Th and Pa favor the fcc structure and U, Np, and Pu favor the bcc structure. Skriver[17] also attempted to calculate the crystal-structure sequence of Ce under pressure (fcc-orthorhombic-bct) but did not quite reproduce the experimental data and it was later shown that a full-potential description was necessary to obtain the required accuracy.[20] Wills, Eriksson, and Boring[20] showed that the crystal-structure sequence of Ce under pressure was correlated with the $4f$, $5d$, and Madelung contributions to the total energy. The present investigation is a similar attempt to account for the crystal structures of the light actinides.

II. DETAILS OF CALCULATIONS

The total energy of the light actinides is on the order of several thousand Ry/atom while the difference in energy between the different crystallographic phases is on the order of a few mRy/atom. Hence, an accurate computational technique is required. We used a full-potential linear-muffin-tin-orbital technique[21,22] in the calculations reported here. Exchange and correlation were treated in the local-density approximation (LDA) using the Hedin-Lundqvist exchange-correlation functional. The calculations were all electron, fully relativistic (spin-orbit coupling included at each variational step[23]), and employed no shape approximation to the charge density or potential. The basis set, charge density, and potential were expanded in spherical harmonic series within nonoverlapping muffin-tin spheres and in Fourier series in the interstitial region between the spheres. The volume in the muffin-tin spheres was set at a fixed fraction (approximately 0.50) of the total volume, for all structures and volumes. This scheme was chosen to make the basis set as consistent as possible in calculating energies at different structures and volumes. The relatively small volume fraction contained in the muffin-tin spheres is that approriate to the α-U structure.

The basis set, comprised of augmented linear muffin-tin orbitals,[23,24] contained $6s$, $6p$, $7s$, $7p$, $6d$, and $5f$ partial waves in a single, fully hybridizing "energy panel." The inclusion of the $6s$ partial wave as a band state rather than as a core state was necessitated by the small size of the muffin-tin spheres. Two sets of energy parameters,[23,24] one with energies appropriate to the semicore $6s$ and $6p$ bands and one with energies corresponding to the valence bands, were used to calculate the radial functions for the expansions of the bases in the muffin-tin spheres. Similarly, three sets of tail parameters (the kinetic energy of the bases in the interstitial[23,24]), corresponding to $6s$, $6p$, and valence energies, were used. Approximate orthogonality between bases with the same l value was maintained by energy separation.

The tails of the basis functions (the extension of the bases outside their parent spheres) were linear combinations of Hankel or Neumann functions with nonzero kinetic energy. The large interstitial volume in the calculations rendered inadequate the use of a single tail function

for each (n,l) basis and two schemes were adapted to improve the quality of the bases in the interstitial region. Most of the calculations reported in this paper were done with a "doubled" basis set consisting of pairs of tail functions having different kinetic energies but otherwise specified by the same set of parameters. This scheme is accurate in that the expansion of the wave functions is converged in the interstitial (as well as in the muffin tins) and the total energy is substantially converged with respect to basis-set size. It is also stable; within broad limits the results are insensitive to the interstitial parameters used and to the choice of muffin-tin radius. In the calculations reported here, the tail parameters were chosen to bracket the energies of the bands for which they were used. The disadvantage is, of course, loss of efficiency with respect to a single basis set.

As a reference, we also performed somewhat less accurate calculations using a single basis set but with the tail functions being fixed linear combination of three Hankel (or Neumann) functions with different kinetic energies. The coefficients were chosen for each (n,l) value by fitting to atomic wave functions calculated from self-consistent potentials; the kinetic energies of the tail functions were chosen to optimize the fit. This scheme retains all the advantages of a minimal basis set while improving the wave functions and the total energy with respect to a single basis set using single tail functions. The results are somewhat sensitive to the parameters used, however, and the total energies are less converged than with the double basis set.

Integration over the Brillouin zone was done using "special-point" sampling.[25] The results reported here used 10–60 points in an irreducible wedge of the fcc Brillouin zone, 16–100 points in an irreducible wedge of the orthorhombic Brillouin zone, and 58–80 points in an irreducible wedge of the body-centered tetragonal zone. The number of points was increased until the total energy did not change. We tested convergence in the bct and orthorhombic phases by performing calculations with distortion parameters set to correspond to the fcc structure. The calculated energies were then the same for all three structures (within 0.03 mRy). Spherical harmonic expansions were carried out through $l=8$ for the bases, charge density, and potential. The Fourier series for the basis functions contained 369 plane waves for the fcc structure, 489 plane waves for the bct structure, and 1053 plane waves for the orthorhombic structure; the Fourier series for the charge density and potential contained 1695 plane waves for the fcc structure, 2255 plane waves for the bct structure, and 5175 plane waves for the orthorhombic structure. The difference in energy between the different structures was converged to less than ~ 0.1 mRy with these expansion sets.

III. TOTAL-ENERGY RESULTS

In this section we discuss our results. In Fig. 2 we show our calculated total energies as a function of
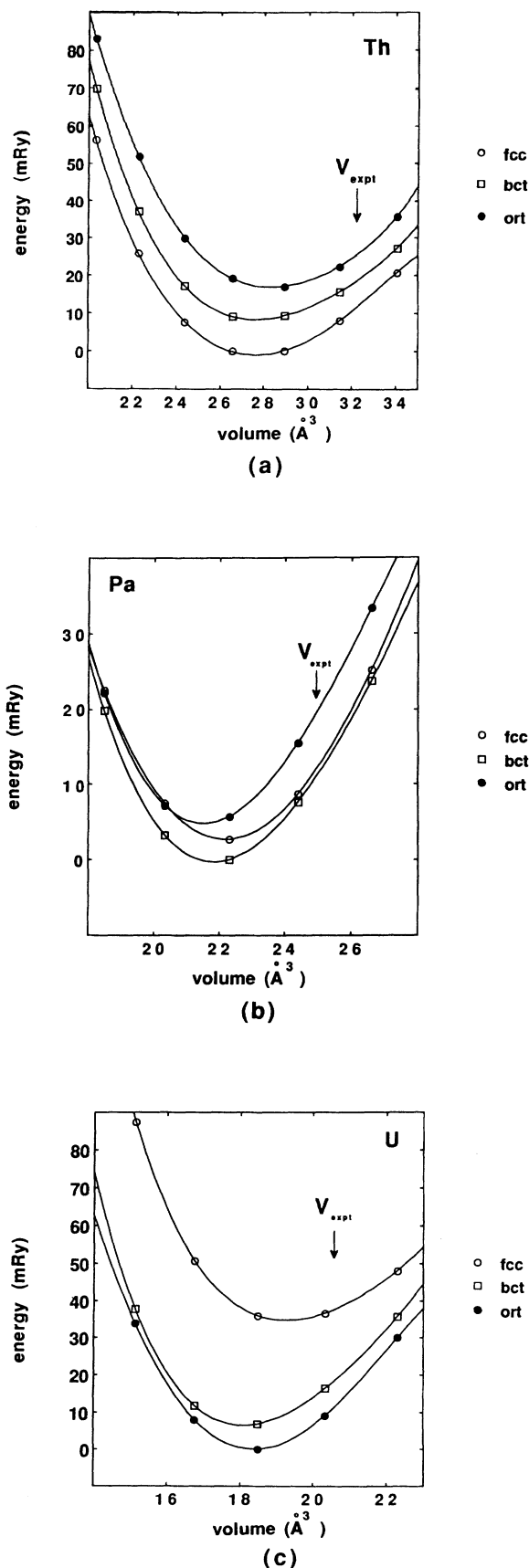

(a)

(b)

(c)

FIG. 2. Calculated total energy as a function of volume for (a) Th, (b) Pa, and (c) U.

volume for (a) Th, (b) Pa, and (c) U. The total energies were calculated for three different crystal structures; fcc, bct, and the face-centered orthorhombic α-U structure. These crystal structures were considered since it is known experimentally that Th crystallizes in the fcc structure, Pa in the bct structure, and U in the α-U structure. The calculated stable crystal structures agree with experiment for each element.

The bct phase of Pa has an (experimental) c/a ratio of about 0.83. We calculated the c/a ratio at the experimental volume to be 0.814; this value was used to obtain the energy curve shown in Fig. 2(b). Since the total energy is fairly insensitive to the value of c/a, we have, therefore, tried to estimate the error in our calculated c/a ratio. We take the resolution of the total-energy differences between different c/a ratios in Fig. 3(a) to be approximately 0.1 mRy; the corresponding value of the c/a ratio for Pa is 0.814 ± 0.005. Furthermore, the orthorhombic α-U structure has two atoms/cell, with atomic positions (0,0,0) and $(1-2y, 1-2y, 0.5)$ in units of the Bravais lattice vectors $(-a/2, 0, c/2)$, $(a/2, 0, c/2)$, and $(0, b, 0)$. The experimental c/a ratio is 2.06 and the b/a ratio is 1.73. We calculated the parameter $2y$ using experimental c/a and b/a ratios at the experimental volume and obtained a value of 0.186; the experimental value of $2y$ is 0.20. The energy as a function of $2y$ is shown in Fig. 3(b). The energy has a fairly strong dependence on this parameter. We used the calculated value of $2y$ together with the experimental values of c/a and b/a to calculate the energy curve shown in Fig. 2(c).

The calculated crystallographic properties, as well as the equilibrium volumes and bulk moduli and their corresponding experimental values, are collected in Table I. Notice that the overall agreement between experiment and theory is fair to good. The equilibrium volumes agree within $\sim 12\%$ (by comparing with the lowest experimental volume of Th in Table I), and the bulk moduli (with the exception of Pa) lie within the limits of the experimental data. This agreement is comparable to that found for the $3d$ elements, and slightly worse than one finds for the $4d$ and $5d$ elements. For instance, the calculated volume of bcc V (a paramagnetic $3d$ transition metal) is $\sim 10\%$ smaller than the experimental one.[26] The notable exception is the disagreement between the calculated and experimental bulk modulus of Pa. The trend in the calculated bulk moduli is consistent with the trend in equilibrium volumes. The experimental bulk modulus is in rather sharp contrast to expectation and, on the whole, we prefer our calculated value.

It is also interesting to note that the agreement between experiment and theory is better for uranium than for thorium, which is essentially an $[spd]$ metal. It has been argued[27] that the local-density approximation overestimates the bonding of f-electron systems. This may indeed be the case; however, the disagreement that we find between calculated and experimental values is similar (albeit slightly exacerbated) to that found in the $3d$ transition series. Based on these results, it would seem that the LDA does not make too much of an exception for f electrons in these elements.

It is evident from Table I that our calculations can ac-

count for most of the ground-state properties of the light actinides, including the crystal structures. It is especially interesting to notice that Th (which is essentially a normal tetravalent $[spd]$ metal) crystallizes in the fcc structure (as do many other normal $[spd]$ metals), whereas the $5f$ metals have a more open bct or orthorhombic structure. One of the motivations for this work is investigating why Pa and U prefer these unique crystal structures. It has been suggested[28] that since the early actinides are part of a $5f$ series, with an itinerant $5f$ band being successively occupied with increasing atomic number, it is the itinerant $5f$ electrons that cause the anomalous struc-
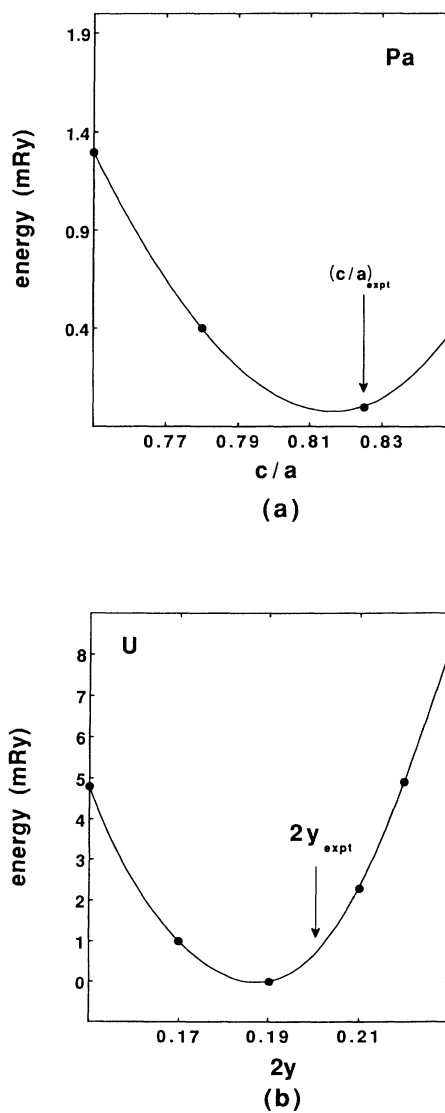

FIG. 3. (a) Calculated total energy as a function of the c/a ratio for bct Pa. The calculation was done at a volume close to the experimental volume. (b) Calculated total energy as a function of the positional parameter $2y$ for α-U. The calculation was done at a volume close to the experimental volume.

tures. One reason for the $5f$ elements to favor distorted structures with directional bonds might be found in the complex spatial shape of the f spherical harmonics. To investigate these ideas, we show in Fig. 4 the $6d$ and $5f$ occupation numbers of Th [Fig 4(a)], Pa [Fig. 4(b)], and U [Fig. 4(c)] as a function of volume. "Occupation number," in the context of our calculations, refers to the integrated l-projected density of states (ignoring the interstitial region). It should be mentioned here that these numbers are not unique since they, to some extent, depend on the muffin-tin radius. However, at the experimental volumes ~97% of the $5f$ radial function lies within the muffin-tin sphere (a plot of this function was

TABLE I. Experimental and theoretical values of the crystal structure, equilibrium volume, bulk modulus, and crystal structure parameters for thorium, protactinium, and uranium.

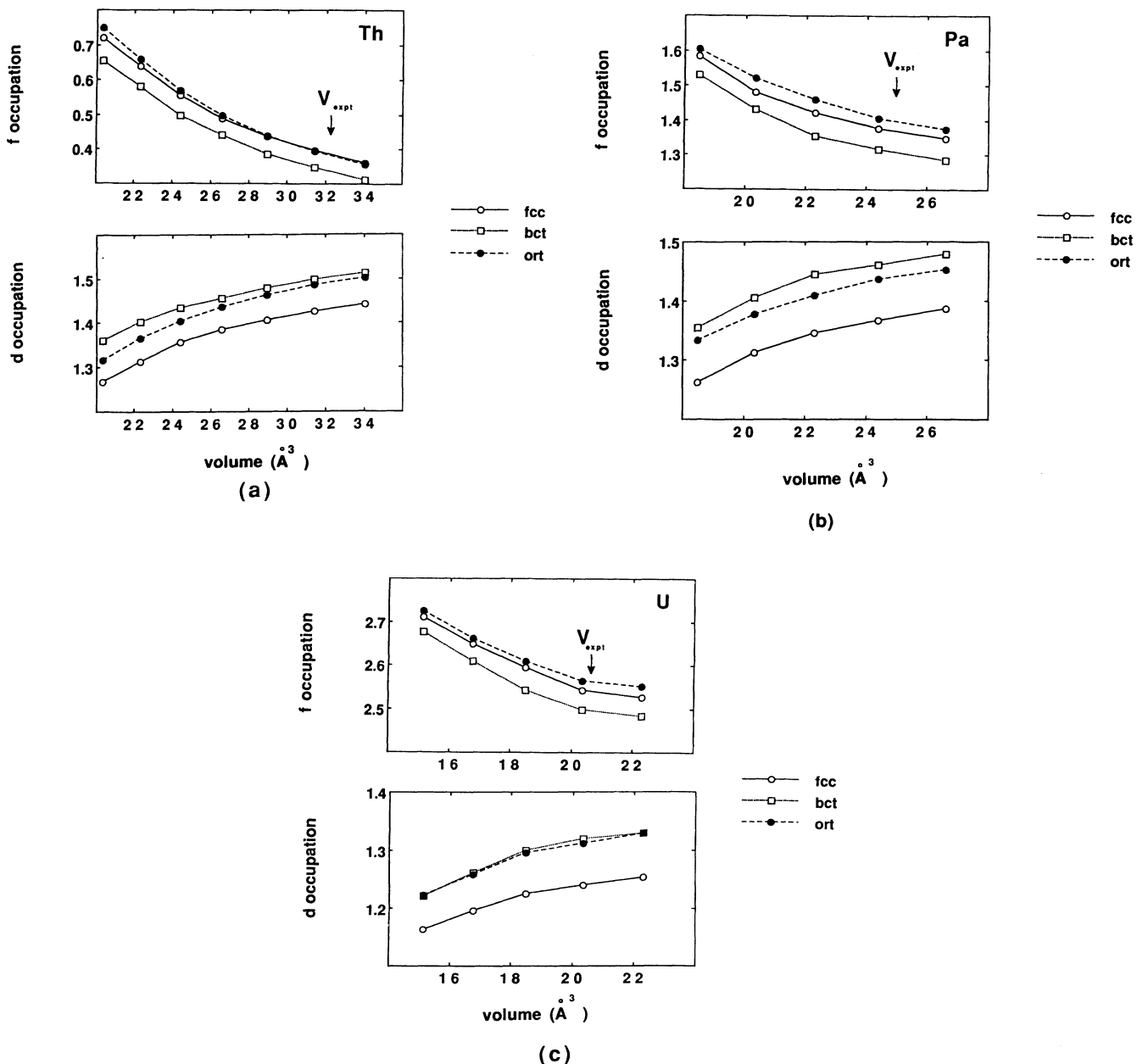|	Th	Pa	U
V_{eq}^{expt} (Å^3)	32.0–33.61	24.94	20.58
V_{eq}^{theor} (Å^3)	27.95	21.91	18.42
B^{expt} (Mbar)	0.40–0.72	1.57	1.01–1.47
B^{theor} (Mbar)	0.42	0.79	1.25
Crystal structure (expt.)	fcc	bct	ort
Crystal structure (theor.)	fcc	bct	ort
Crystal parameter (expt.)		$c/a = 0.825$	$2y = 0.202$
Crystal parameter (theor.)		$c/a = 0.814$	$2y = 0.186$

FIG. 4. Calculated occupation numbers ($6d$ and $5f$) for (a) Th, (b) Pa, and (c) U.

published by Koelling[15]), making this number very in-sensitive to the choice of the muffin-tin radius. Notice that the 5f occupation increases with about one electron when going from one element to another, and that there is an [spd]→f transfer with decreasing volume.[29] In Fig. 4 we see that Th, at ambient pressure, is essentially a nor-mal tetravalent [spd] metal, which is consistent with its close-packed structure. However, it should be noticed that the ∼0.4 5f electron does play a non-negligible role. The crystal structure of Th is fcc as opposed to "normal" tetravalent systems (Ti, Zr, and Hf) that crystallize in the hcp structure. Also, the calculated equilibrium volume of Th is in poor agreement with experiment if the 5f elec-trons are neglected,[4] as is the Fermi-surface topology.[15] For Pa and U, the 5f occupation becomes a larger frac-tion of the number of valence electrons, suggesting that the 5f electrons do influence the anomalous crystal struc-tures found for these elements. Notice also that the occu-pation numbers are different for different crystal struc-tures.

To illustrate the importance of the 5f electrons more clearly we show, in Fig. 5, the calculated energies of the orthorhombic and bct structures relative to the fcc struc-ture as a function of element (and, therefore, 5f occupa-tion), at the experimental volume (at these volumes Th has ∼0.4 5f electron, Pa ∼1.3 5f electrons, and U∼2.6 5f electrons). Figure 5 shows that there is a clear corre-lation between the open structures becoming lower in en-ergy and increasing 5f occupation.

Further evidence that the 5f electrons are responsible for the more open, less symmetric structures is obtained from a calculation of the energy of uranium omitting the 5f partial wave from the basis set. This (self-consistent) calculation used only s, p, and d partial waves but had the correct number of valence electrons (6). The total energy was found to be about 16 eV higher than the calculation
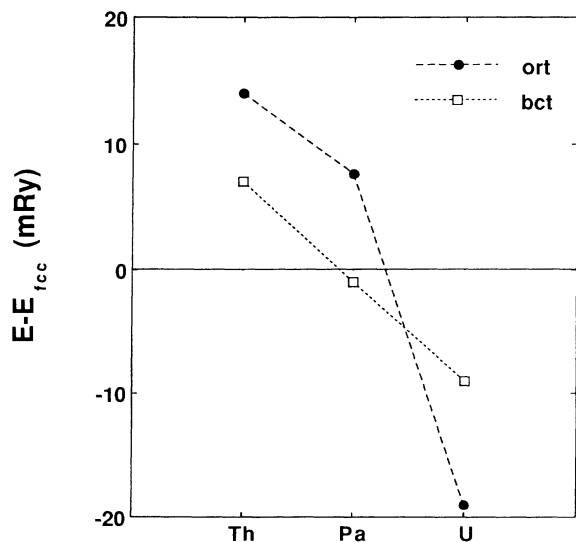
with 5f orbitals, and the wrong crystal structure is then found to be stable; the fcc structure is lowest in energy, with both the bct and α-U structure about 30 mRy higher per atom.

IV. ELECTRONIC STRUCTURE

In this section we discuss the underlying electronic structure for the three elements in the three crystal struc-tures. In Fig. 6 we show the calculated density of states (DOS) (at the experimental volume) for Th [Fig. 6(a)], Pa [Fig. 6(b)], and U [Fig. 6(c)], in the three different crystal structures. The upper curve is the total DOS, whereas the shaded area represents the 5f partial DOS. The l-projected DOS have been scaled so that their sum is equal to the total DOS, thereby including the interstitial contribution. The face-centered orthorhombic structure (α-U) has two atoms/cell, but since the partial DOS for the two atoms are almost identical we show only one of them. Notice that the 5f partial DOS dominates the overall features, for all elements in all three structures. Notice that the width of the 5f band is more or less the same for the three elements. This comes about from two competing effects that nearly cancel each other. Namely, due to incomplete screening effects one would, for a con-stant volume, expect the bandwidth to become narrower for the heavier elements. This effect is counterbalanced by the fact that the volume decreases with increasing atomic number, giving larger 5f overlap and a broaden-ing of the bands. Furthermore, Fig. 6 shows that the width of the DOS for the three different structures is ap-proximately the same. The details of the DOS vary, but the general trend is that the structures with higher sym-metry show sharper features in the DOS. For the low-symmetry structures the sharp van Hoove singularities become smeared out. Notice also in Fig. 6 that, from the DOS, it is hard to argue why uranium should favor the orthorhombic structure and thorium the fcc structure (other than observing that the 5f band is almost empty in Th and becomes gradually filled for Pa and U). Further-more, Fig. 6 suggests that the electronic structure of the three different structures is associated with metallic bonding.

In Fig. 7 we show the energy bands for fcc Th [Fig. 7(a)], bct Pa [Fig. 7(b)], and α-U [Fig. 7(c)]. The bands were computed at the experimental volume (upper panel) and at ∼15% compressed volume (lower panel). Notice that there is a broadening of the bands with decreasing volume. One can also distinguish a relative shift of bands with different l character (Fig. 7). For instance, the lowest eigenvalue at the Γ point (an s state) in bct Pa moves up with decreasing volume, whereas the lowest ei-genvalue at the X point (a d state) moves down. Similar-ly, the eigenvalue at the Γ point in fcc Th is almost in-sensitive to volume, whereas the eigenvalue at the X point moves down with decreasing volume.

V. CHARGE-DENSITY CONTOURS

Charge-density contour plots are shown in Figs. 8–10. Here we display the charge densities for the three ele-ments in their experimentally observed crystal structures;

FIG. 5. Calculated energy difference between fcc (which is the reference level, =0), the bct, and the α-U structure for Th, Pa, and U.

fcc Th (Fig. 8), bct Pa (Fig. 9), and orthorhombic U (Fig. 10). The Th plot represents a cut in the (100) plane, the Pa plot a cut in the (110) plane, and the U plot a cut in the (100) and a cut in the (010) plane. We plot both the total density [Figs. 8(a), 9(a), 10(a), and 10(c)] as well as the nonspherical component, i.e., the density obtained when the spherical component is subtracted from the total density inside the muffin-tin spheres and the planar average is subtracted from the interstitial. The density so obtained is shown in Figs. 8(b), 9(b), 10(b), and 10(d). Notice that since the average interstitial density does not

equal the spherical component at the muffin-tin radius, there will be a "step" in the nonspherical density, which of course is absent in the total density.

The Th density is characterized by spherical regions centered around each atom site, with a symmetric density in the interstitial region. Although the nonspherical component is rather small for Th, there is still a tendency for directionality in the charge density. The Pa charge-density contour also shows spherical regions around each lattice site. The density in the interstitial region is less symmetric and more directional than for Th, and the
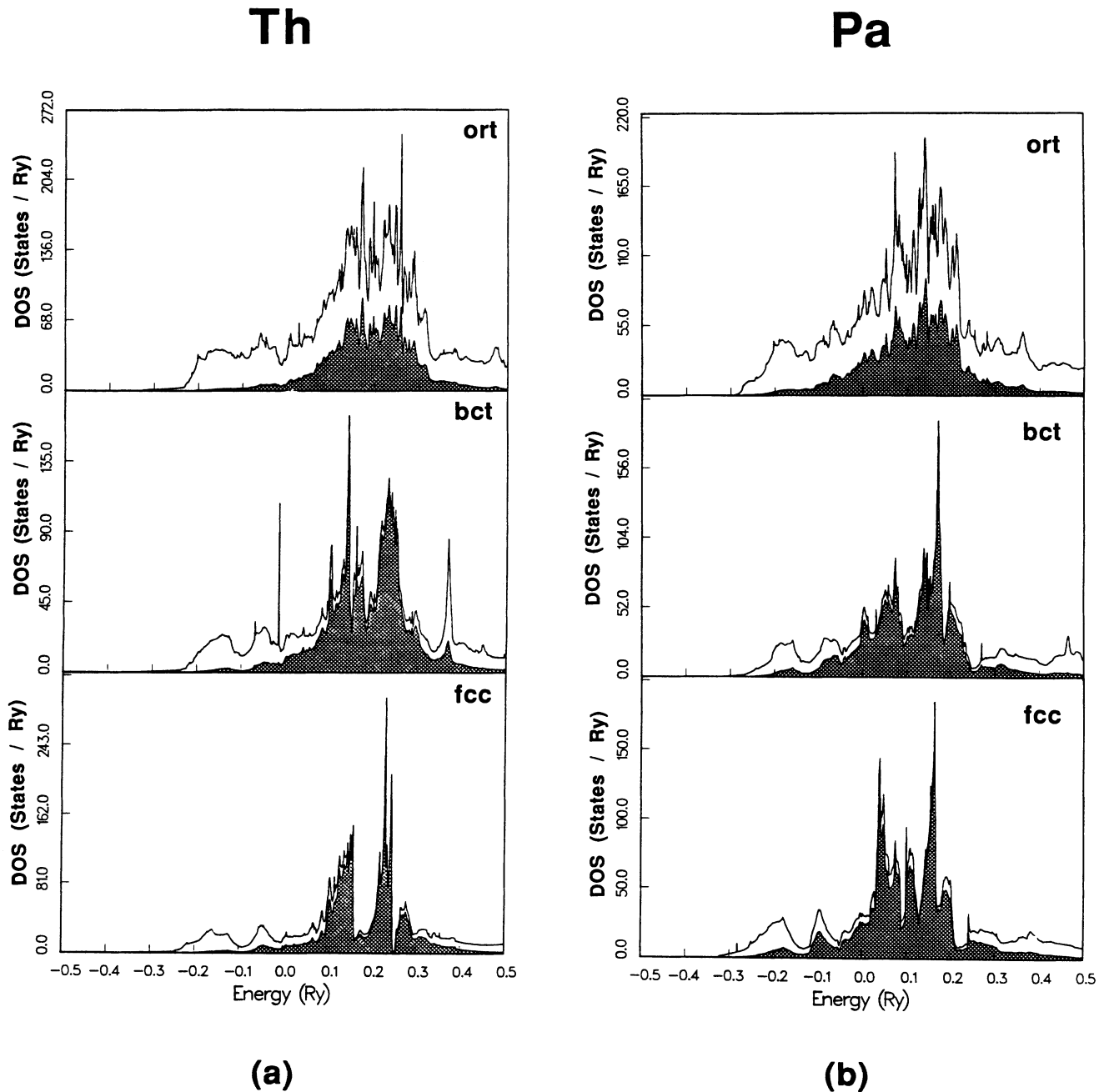

FIG. 6. Density of states (DOS) for (a) Th, (b) Pa, and (c) U in the three crystal structures; fcc (lower curve), bct (middle curve), and orthorhombic (upper curve). Energies are in electron volts and the Fermi level is at zero. The upper curve in each panel represents the total DOS and the shaded area the $5f$ partial DOS.

nonspherical component inside the muffin-tin spheres is more pronounced. For instance, there are lobes of charge density inside the muffin-tin spheres which point in the direction of the nearest neighbors, along the [001] direction. Finally, we notice that for U the charge density is quite anisotropic both in the interstitial region as well as inside the muffin-tin spheres. This can be seen by comparing the charge densities cut along the different crystal planes (010) [Figs. 10(a) and 10(b)] and (100) [Figs. 10(c) and 10(d)]. Notice that the charge density in the interstitial is higher in the (010) plane. Notice also that the cut in the (100) plane shows spherical regions of the charge density in the interstitial region. This is simply a reflection of the charge density associated with the atoms

U

(c)

FIG. 6. (Continued).

lying one plane below the plane in which the cut was made.

The density contour plots shown in Figs. 8–10 reveal the large degree of nonsphericity in the charge densities of the more open structures. It is tempting to infer, from these figures, that the increased nonsphericity is arising from the f states, but this would be a mistake. The charge density of Th in the α-U structure (not shown) and the charge density of α-U calculated without $5f$ states in the basis (not shown) are very similar to the charge densities shown in Fig. 10. To understand the preference for open structures as $5f$ occupation increases, we reason as follows. The nonsphericity is associated with covalent bonding, hence a crystal may gain covalent energy by forming in a more open structure. This energy is gained, however, at the expense of Madelung energy; the Madelung term in the energy favors structures of high symmetry. For a crystal to prefer the open structures, the gain in energy from covalent bonding must be larger than the cost in Madelung energy. The gain in covalent energy in going from high- to low-symmetry structures will be greatest for bands with a large degree of degeneracy at the Fermi energy, since breaking the degeneracies by lowering the symmetry will result in lower-energy occupied states and higher-energy unoccupied states. The gain in energy will be greater the larger the density of states at the Fermi energy. The $5f$ states form a set of bands of high degeneracy clustered around the Fermi energy, and the density of states at the Fermi energy increases as a function of $5f$ occupation; hence the tendency for open structures will increase as the $5f$ count increases. As evidence that this is the mechanism driving the increasing stability of open structures, we note that, although the charge-density contours of α-U calculated as an $[spd]$ metal (not shown) are very similar to Fig. 10, it is the fcc structure that is stable when U is treated as an $[spd]$ material. This mechanism also drives the $\alpha \rightarrow \alpha'$ transition in Ce.[20]

Because the $5f$-band width in U (about 3 eV) is approximately the same as the $3d$-band width in Ni, it is interesting to compare their crystal structures, orthorhombic and fcc, respectively. If the only driving force for the open structures is a narrow band pinned at E_F one would expect a similar structure also for Ni. However this is not the case, and clearly the character of the narrow band (f or d) plays an important role. The f systems lower their energy by adopting low-symmetry structures, similar to the behavior of Mn, whereas most of the latter $3d$ systems (e.g., Fe, Co, and Ni) become magnetic. This might be explained by the fact that the calculated d exchange integrals (I_{dd}) for the late $3d$ elements is almost twice as large as the f exchange integrals (I_{ff}) for the early actinides.[30]
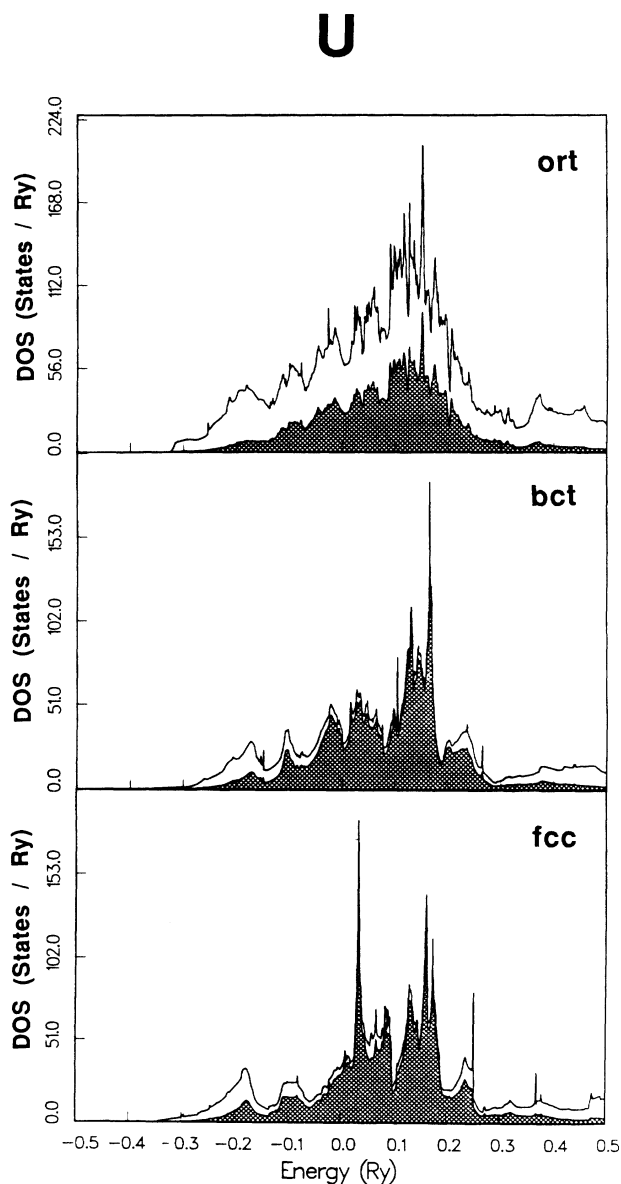
VI. fcc CALCULATION

A common approximation for calculating equilibrium volumes of elements with open, complicated structures is to assume a much simpler structure (say, fcc), and then calculate the total energy versus volume for this simplified problem. This approach was used in Refs. 4
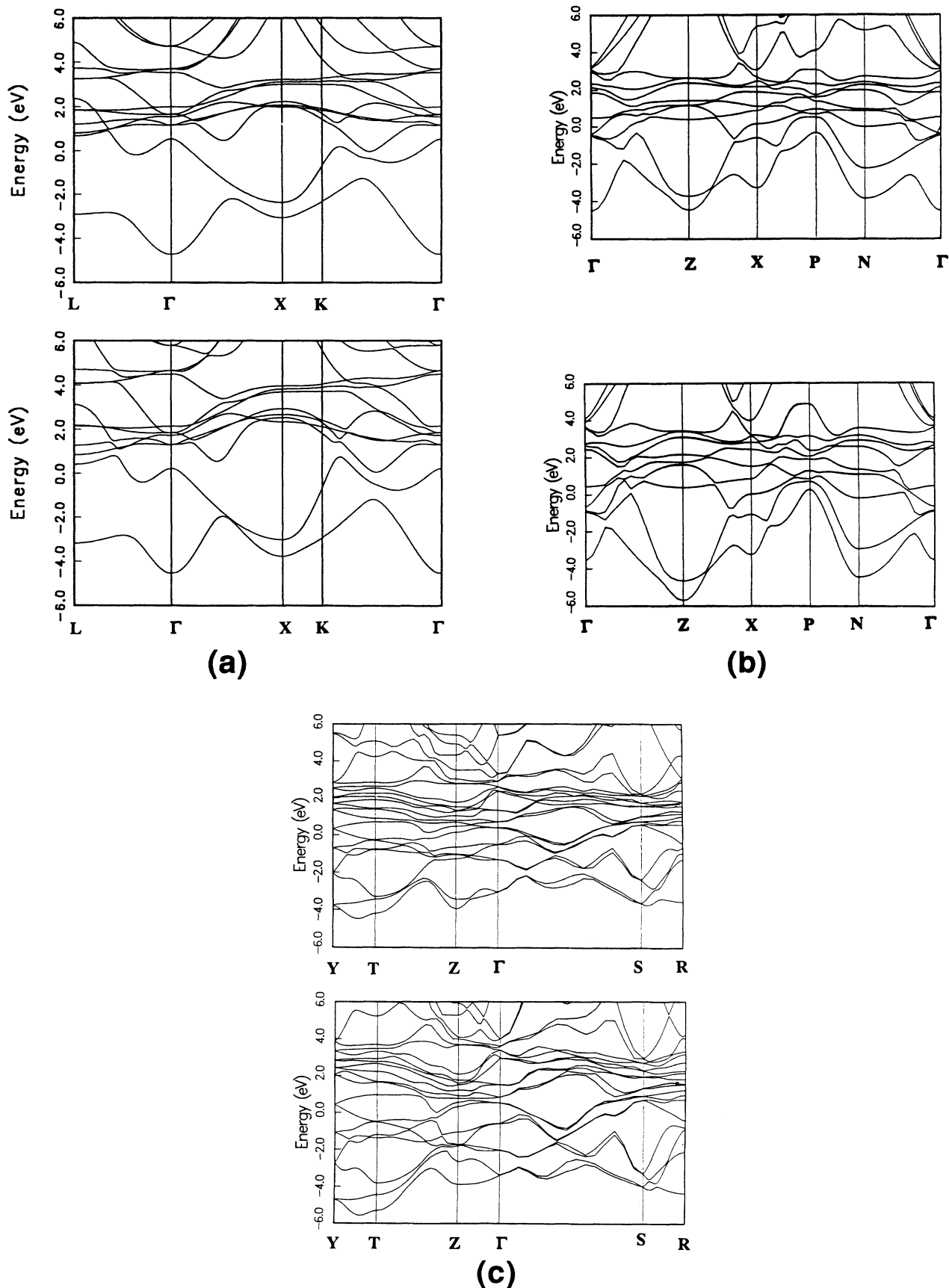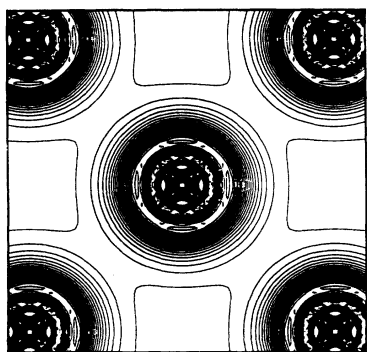
(a)

(b)

(c)

FIG. 7. Calculated energy bands for (a) Th fcc, (b) Pa bct, and (c) α-U. The bands were computed at the experimental volume (upper panel) and at $\sim 15\%$ compressed volume (lower panel). Energies are in electron volts and E_F is at zero.
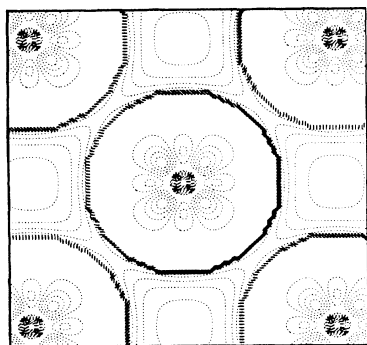
and 10–13. The argument for the validity of this approximation is that the energy difference between structures is much smaller than the energy of cohesion. However, the present work shows that the energy difference between a hypothetical fcc structure and the true crystal structure can be substantial, and it is, therefore, interesting to investigate the validity of the above-mentioned approach for calculations of the equilibrium volumes of the light actinides. We have therefore calculated (using the "single" basis set described in Sec. II) the equilibrium volumes in the fcc structure of the light actinides Th, Pa, U, Np, and Pu, and, for comparison, Th, Pa, and U in their true structures. In Fig. 11 we show these volumes together with experimental data. [The single basis calculation gives slightly larger equilibrium volumes than the double basis (see Table I)]. Notice that the deviation between the volumes in the true structure and the fcc phase is larger for uranium than protactinium. This seems to indicate that for the more open structures the fcc calculation becomes less accurate, an expected result. Unfortunately we have at the present time no theoretical data

for Np and Pu in their true crystal structures but, since these structures are very open, we expect a large discrepancy between their equilibrium volumes and the fcc data shown in Fig. 11. Despite the crudeness of assuming a fcc structure for the light actinides, it is interesting to note that the general agreement between experiment and theory is quite good. The parabolic behavior is well reproduced in our fcc calculations, an effect caused by the successive filling of the $5f$ band.[10-12] The largest disagreement between our fcc volumes and experiment is found for Pu. This was also found by Skriver et al.[10] using the linear-muffin-tin-orbital method in the atomic-sphere approximation (ASA). However the calculation presented in Ref. 10 was scalar relativistic, omitting spin-orbit coupling. The relatively large disagreement between the scalar-relativistic volume[10] and experiment was argued to be caused by the spin-orbit coupling, since Brooks[11,12] found that a fully relativistic ASA calculation (assuming the fcc structure) gave much better agreement with experiment. Thus it was deduced that the enhanced volume of Pu, relative to Np, is caused by relativistic effects.[11,12] However, the present investigation (which is fully relativistic and does not rely on the ASA) does not reproduce the upturn at Pu, but gives a volume similar to the results of Skriver, Johansson, and Andersen.[10] We therefore believe that the upturn for Pu is caused by the very anomalous crystal structure, a speculation which we plan to investigate in the near future by calculating the equation of state of α-Pu.
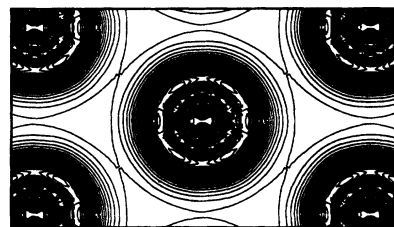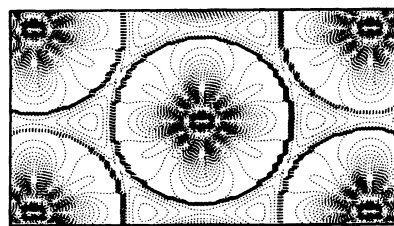
Th(100)

(a)

(b)

FIG. 8. Charge-density contours (in units of $e^-/\text{a.u.}^3$) for fcc Th. The density is for a fcc crystal cut in the (100) plane. The total density is shown in (a) and the nonspherical density is shown in (b). The spacing between the full-drawn lines is 0.01 (a), and between the dotted lines 0.002 (b).
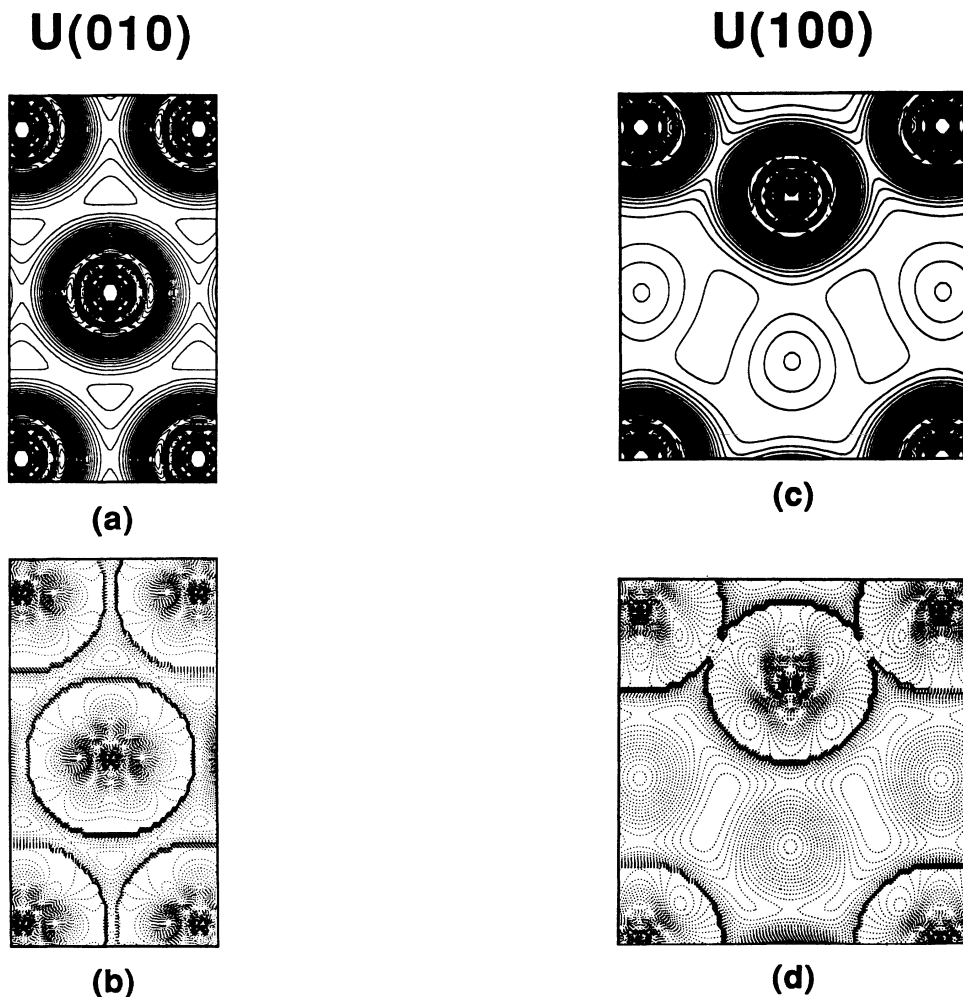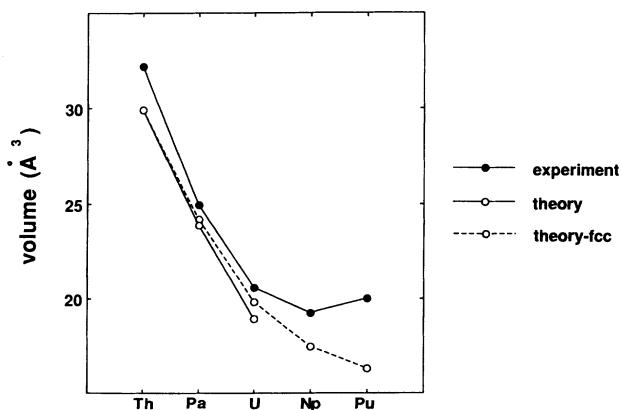
Pa(110)

(a)

(b)

FIG. 9. Charge-density contours (in units of $e^-/\text{a.u.}^3$) for bct Pa. The density is for a bct crystal cut in the (110) plane. The total density is shown in (a) and the nonspherical density is shown in (b). The spacing between the full-drawn lines is (a) 0.01, and between the dotted lines (b) 0.002.

U(010)

U(100)

(a)

(b)

(c)

(d)

FIG. 10. Charge-density contours (in units of e^-/a.u.^{3}) for α-U. The density is for an orthorhombic crystal cut in the (010) and (100) plane. The total density cut in the (010) plane is shown in (a) and the corresponding nonspherical density is shown in (b). The total density cut in the (100) plane is shown in (c) and the corresponding nonspherical density is shown in (d). The spacing between the full-drawn lines is (a),(c) 0.01, and between the dotted lines (b),(d) 0.002.

FIG. 11. Calculated equilibrium volumes of the light actinides using the true crystal structure (open circles, full-drawn lines), and a hypothetical fcc structure (open circles, dashed lines). Also quoted are the experimental volumes (filled circles, full-drawn lines).

To further investigate the effects of spin-orbit coupling on the equation of state, we also performed scalar-relativistic calculations (omitting the spin-orbit coupling) for U and Pu. In both cases we obtained equilibrium volumes that were about 5% *larger* than those resulting from the fully relativistic calculations. This result is opposite to the arguments of Brooks.[11,12] However, our calculations did include the $6p$ states in the valence band, whereas these states were considered as core states in the calculations presented in Refs. 11 and 12. Treating the $6p$ states in a scalar-relativistic framework is quite different from a fully relativistic one, since the spin-orbit coupling pushes up the $6p_{3/2}$ subband closer to E_F, thereby increasing the interaction (hybridization) with the valence states. Therefore, we attribute the 5% increase in the scalar-relativistic case to the difference in treating the $6p$ states.

VII. CONCLUSION

The crystal structures, equilibrium volumes, and bulk moduli have been calculated from first principles for the

light actinides. The general agreement with experiment is good, except for the bulk modulus for Pa. We have shown that the distorted crystal structures found for the $5f$ elements are correlated with $5f$ occupation and the gain in energy resulting from $5f$ covalent bonding. When explicitly neglecting the $5f$ contribution to the bonding we have shown that the crystal structure of U cannot be explained. We also find that for U the energy difference between a hypothetical fcc structure and the true crystal structure is about 0.5 eV. This is a quite substantial value, in relation to, for instance, the cohesive energy.[11,12]

The calculated volumes of the light actinides (Th–Pu), in a hypothetical fcc structure resemble the experimental data rather well, with the worst agreement found for Pu. Contrary to earlier work[11,12] we cannot, using a simple fcc structure, explain the enhanced volume of Pu relative to Np. Before any conclusion can be drawn, calculations of an equation of state for α-Pu (16 atoms/unit cell) must be performed. We plan to do this in the future.

The general picture of the light actinides is supported by the present investigation, namely, the $5f$ wave func-tions overlap and form a narrow band (2–3-eV broad), pinned at E_F. This narrow band hybridizes with the rest of the valence orbitals. The parabolic behavior of the volumes can then be understood, using a simple Friedel model, from the gradual filling of this $5f$ band. Also, shown in the present work, the gradual filling of the $5f$ band drives the crystal structures from the symmetric fcc structure (found for Th) to the more open, less symmetric face-centered orthorhombic structure (found for α-U). We argue that the open, less symmetric, structures are stabilized by the narrow $5f$ band, which is pinned at E_F.

ACKNOWLEDGMENTS

[1]G. T. Seaborg, Chem. Eng. News **23**, 2190 (1945).

[2]W. H. Zachariasen, Acta Crystallogr. **5**, 19 (1952); W. H. Zachariasen, *The Metal Plutonium*, edited by A. S. Coffinbery and W. N. Miner (University Of Chicago Press, Chicago, 1961).

[3]See articles in *Handbook on the Physics and Chemistry of the Actinides*, edited by A. J. Freeman and G. H. Lander (North-Holland, Amsterdam, 1984).

[4]A theoretical calculation and quoted experimental data can be found in P. Söderlind, L. Nordström, Lou Yongming, and B. Johansson, Phys. Rev. B **42**, 4544 (1990).

[5]G. M. Mayer, Phys. Rev. **60**, 184 (1941).

[6]E. A. Kmetko and H. H. Hill, in *Plutonium 1970 and Other Actinides*, edited by W. N. Miner (AIME, New York, 1970), p. 233; A. J. Freeman and D. D. Koelling, in *The Actinides: Electronic Structure and Related Properties*, edited by A. J. Freeman and J. E. Darby (Academic, New York, 1974), Vol. 1, p. 51.

[7]B. Johansson, Phys. Rev. B **11**, 2740 (1975).

[8]B. Johansson and A. Rosengren Phys. Rev. B **11**, 2836 (1975); A. Rosengren and B. Johansson, *ibid.* **26**, 3068 (1982).

[9]J. L. Smith and R. Haire, Science **200**, 535 (1978).

[10]H. L. Skriver, B. Johansson, and O. K. Andersen, Phys. Rev. Lett. **41**, 42 (1978); **44**, 1230 (1980).

[11]M. S. S. Brooks, J. Magn. Magn. Mater. **29**, 257 (1982); J. Phys. F **13**, 103 (1983).

[12]S. S. Brooks, J. Phys. F **13**, 103 (1983); M. S. S. Brooks, B. Johansson, and H. L. Skriver, *Handbook on the Physics and Chemistry of the Actinides* (Ref. 3), Chap. 3, p. 153.

[13]H. L. Skriver, O. Eriksson, I. Mertig, and E. Mrosan, Phys. Rev. B **37**, 1706 (1988).

[14]R. C. Albers, A. M. Boring, L. E. Cox, and O. Eriksson (un-published).

[15]D. D. Koelling, J. Phys. (Paris) Colloq. **40**, C4-117 (1979).

[16]J. Shirber, A. J. Arko and E. S. Fischer, Solid State Commun. **17**, 533 (1975).

[17]H. L. Skriver, Phys. Rev. B **31**, 1909 (1985).

[18]J. C. Duthie and D. G. Pettifor, Phys. Rev. Lett. **38**, 564 (1977).

[19]G. W. Fernando, R. E. Watson, M. Weinert, Y. J. Wang, and J. W. Davenport, Phys. Rev. B **41**, 11 813 (1990); R. E. Watson, G. W. Fernando, M. Weinert, Y. J. Wang, and J. W. Davenport, *ibid.* **43**, 1455 (1991).

[20]J. M. Wills, O. Eriksson, and A. M. Boring, Phys. Rev. Lett. **67**, 2215 (1991).

[21]J. M. Wills and B. R. Cooper, Phys. Rev. B **36**, 3809 (1987).

[22]D. L. Price and B. R. Cooper, Phys. Rev. B **39**, 4945 (1989).

[23]O. K. Anderson, Phys. Rev. B **12**, 3060 (1975).

[24]H. L. Skriver, *The LMTO Method* (Springer, Berlin, 1984).

[25]D. J. Chadi and M. L. Cohen, Phys. Rev. B **8**, 5747 (1973); S. Froyen, *ibid.* **39**, 3168 (1989).

[26]This was obtained using the present full-potential code. This result is in agreement with the data published in V. L. Morruzi, J. F. Janak, and A. R. Williams, *Calculated Electronic Properties of Metals* (Pergamon, New York, 1978).

[27]B. I. Min, H. J. F. Jansen, T. Oguchi, and A. J. Freeman, Phys. Rev. B **34**, 369 (1986).

[28]H. H. Hill (unpublished).

[29]The increase in higher-angular-momentum partial waves with decreasing volume is a well-known effect from studies of [spd] metals, where it is referred to as an $s \to d$ transfer [A. K. McMahan, H. L. Skriver, and B. J. Johansson, Phys. Rev. B **23**, 5016 (1981)].

[30]M. S. S. Brooks and B. Johansson, J. Phys. F **13**, L197 (1983).
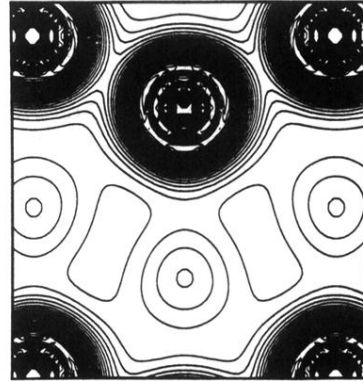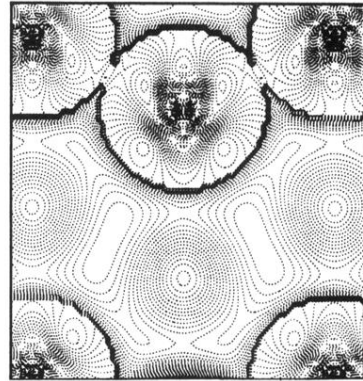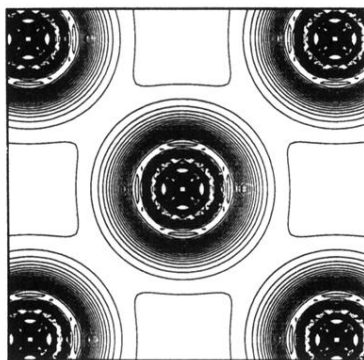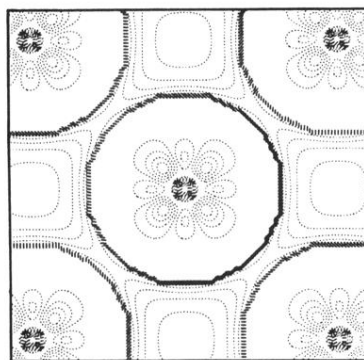
U(010)
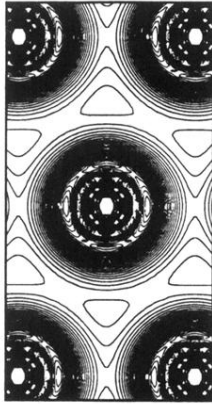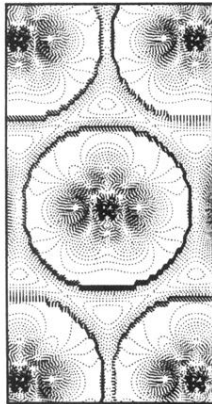
U(100)

(a)

(b)

(c)

(d)

FIG. 10. Charge-density contours (in units of e^-/a.u.^{3}) for α-U. The density is for an orthorhombic crystal cut in the (010) and (100) plane. The total density cut in the (010) plane is shown in (a) and the corresponding nonspherical density is shown in (b). The total density cut in the (100) plane is shown in (c) and the corresponding nonspherical density is shown in (d). The spacing between the full-drawn lines is (a),(c) 0.01, and between the dotted lines (b),(d) 0.002.
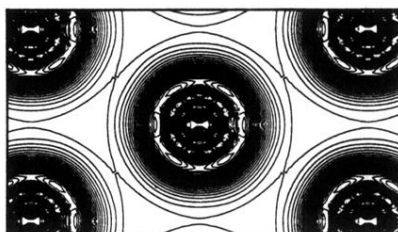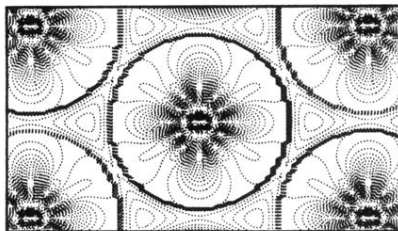
Th(100)

(a)

(b)

FIG. 8. Charge-density contours (in units of $e^-/\text{a.u.}^3$) for fcc Th. The density is for a fcc crystal cut in the (100) plane. The total density is shown in (a) and the nonspherical density is shown in (b). The spacing between the full-drawn lines is 0.01 (a), and between the dotted lines 0.002 (b).

Pa(110)

(a)

(b)

FIG. 9. Charge-density contours (in units of e^-/a.u.^{3}) for bct Pa. The density is for a bct crystal cut in the (110) plane. The total density is shown in (a) and the nonspherical density is shown in (b). The spacing between the full-drawn lines is (a) 0.01, and between the dotted lines (b) 0.002.